Macromol. Symp. **2008**, 273, 73–79

DOI: 10.1002/masy.200851310

# Thermoreversible Poly(vinylidene fluoride) Gels: A Precursor to Multiporous Polymeric Materials

*D. Dasgupta,*[1] J. M. Guenet,[1] A. K. Nandi[2]*

**Summary:** The thermodynamics of gelation of poly(vinylidene fluoride)(PVF$_2$) with camphor (CP) and ethylene carbonate (EC) suggest polymer-solvent compound formation. The presence of solvent molecules in the polymer crystalline phase of the gel is accordingly shown by wide angle X-ray diffraction studies. The dried gels exhibit porous network morphology. Thermoreversible gel of PVF$_2$ in diethyl azelate is also exploited to create multiporous polymer foam. Porosity measurements with the dried PVF$_2$ gels using Mercury intrusion porosimetry and nitrogen sorption ensure the presence of macro and mesopores in the same matrix although the mesoporosity in dried PVF$_2$-CP gels strongly depend on method of drying.

**Keywords:** crystalline phase; gelation; mercury intrusion porosimetry; mesoporosity; polymer-solvent compound

## Introduction

Poly(vinylidene fluoride)(PVF$_2$) is a semicrystalline fluoropolymer which can form gels in solvents containing ester or keto functional groups.[1–3] These gels are thermoreversible in nature and the gelation occurs as a consequence of specific non-covalent interactions operating between the $>CF_2$ dipole of PVF$_2$ and $>C{=}O$ group of the gelator molecules. This type of polymer-solvent organization prevents the polymer chains to get folded to form the infinite spherulitic crystals. Instead, a fibrillar type of crystals are formed to create the junction zones in the gel.[4] Thus, on heating, these crystalline junctions melt giving rise to 'sol state' and on cooling they crystallize producing a 'interlocked net' like morphology wherein a large amount of solvent molecules remain immobilized. Apart from these intercalated solvents housed in the crystalline phase, a good amount of solvents are also located within the swelled network structure of polymer and these solvents have definitely no role in polymer-solvent complex formation. Thus, a successful removal of solvents from the crystalline phase can give rise to nano-voids and at the same time those located in between the network can be taken away to import macropores within the PVF$_2$ xerogel. Formation of similar emptied intercalates of syndiotactic polystyrene have recently been reported.[5–7] In this contribution, we have established this methodology to get multiporous PVF$_2$ using three different solvents namely diethyl azelate (DEAZ), camphor (CP) and ethylene carbonate (EC).

In past few years, there have been many research devoted to the synthesis and design of materials exhibiting multiscale porosity.[8–15] For many applications such as size exclusion chromatography, drug release etc materials having both nano and macropores in the same matrix are necessary.[16] There are many reports of multimodal porosity among the ceramic monoliths[10,14,15] but multiporous polymeric materials are still a few. Due to the presence of nanofibrils, the surface to volume ratio gets increased in the xerogel compared to that of pristine

---

[1] Institut Charles Sadron, CNRS - UPR 22, 23 rue du Loess, BP 84047 67034 Strasbourg Cedex 2, France
E-mail: dasgupta@ics.u-strasbg.fr
[2] Polymer Science Unit, Indian Association for the Cultivation of Science, Jadavpur, Kolkata – 700 032, India

$PVF_2$, encouraging one to use it as catalytic support for suitable substrate–reagent combination. Multiporous $PVF_2$ is of particular interest in making membranes as well because of the extraordinary chemical resistance of $PVF_2$.

$PVF_2$ exhibits complex polymorphic behaviour with five possible crystalline phases namely, $\alpha$, $\beta$, $\gamma$, $\delta$ and $\varepsilon$.[17] The most important polymorph is 'Form-I' or $\beta$ for its polar $TTG\overline{G}$ conformation attributing to piezoelectric and pyroelectric properties. Piezoelectric polymers are increasingly considered as favourable materials for microactuator applications due to their fast response, low operating voltages and greater efficiencies of operation.[18] Here, the $PVF_2$-EC system deserves some discussion as this, to the best of our knowledge, is the first $PVF_2$ gel where, the $\beta$ polymorph of $PVF_2$ is stabilized in the gel state.

Thus, the present paper provides an overview of gelation behaviour of $PVF_2$ in some new solvents and at the same time explores the possibility of using these thermoreversible gels as a template for multiporous polymeric materials.

## Porous Structures of Dried $PVF_2$ Gels

In Figure 1, the surface morphology of different $PVF_2$ gels, as observed in FESEM, are presented. Figure 1a illustrates the nanofibrils present in cyclohexane dried $PVF_2$-DEAZ gel. Figure 1b along with the insets manifests the morphology of cyclohexane dried $PVF_2$-CP gel ($W_{PVF2} = 0.20$) in different length scales. Pores of average diameter around 10 μm are clearly seen and they resemble honey-comb structure (inset of Figure 1b: bottom). At the same time, the inner surfaces of these large macropores contain much smaller pores with a broad size distribution. On further magnification, one can see fibrils (inset of Figure 1b: top). The morphology of cyclohexane dried $PVF_2$-EC gel (Figure 1c) again shows the presence of macroporous network with hierarchical nanoporous structure (inset of Figure 1c).

At this point of discussion, the meaning of 'cyclohexane drying' should be clarified. The $PVF_2$ gels are de-solvated by allowing the dispersion phase (solvent) of the gel to be diffused out in another guest solvent, preferably used cyclohexane. This essentially yields a material wetted with cyclohexane, where the native gel network is well preserved. Finally, the porous material is obtained after evaporation of highly volatile cyclohexane under ambient condition. Since, cyclohexane contains no functional group, it does not have any propensity to induce an additional complexation with $PVF_2$. Of course, the efficiency of such drying technique depends on the solubility parameters of the non polymeric counterpart of gel in cyclohexane and the strength of polymer-solvent interaction as well.

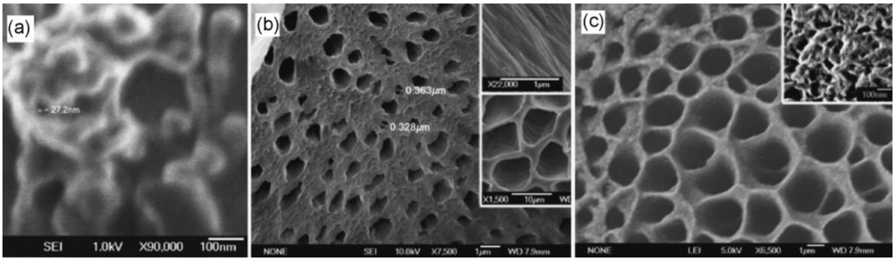

**Figure 1.**
FESEM micrographs of (a) cyclohexane dried $PVF_2$-DEAZ gel ($W_{PVF2} = 0.10$) (b) cyclohexane dried $PVF_2$-CP gel ($W_{PVF2} = 0.20$) [inset: micrographs of the same sample in different magnifications] (c) cyclohexane dried gel of $PVF_2$-EC ($W_{PVF2} = 0.30$).

## Polymer Solvent Complexation

$PVF_2$ forms transparent self-supported soft material when heated with diethyl azelate at 210 °C followed by quenching to room temperature. The phase diagram indicates the formation of incongruently melting compound as reported by Dikshit et al.[2]

We found that in case of $PVF_2$-camphor binary gel, the phase diagram is rather complicated (Figure 2a). Two incongruently melting compounds namely $C_1$ and $C_2$ were identified. The non-variant event at $T = 142$ °C is likely to be a *metatectic* transition when $C_2$ gets transformed into a solid phase $S_{P2}$ which is mixture of thick $PVF_2$ crystals and camphor. The non-variant event at $T = 145$ °C is most probably a eutectic transition where solid phase $S_{P2}$ gives a polymer solution while leaving solid solution $S_{cp}$, remains. The latter consists mainly of camphor molecules wherein $PVF_2$ molecules are embedded. The formation of $PVF_2$-CP molecular compounds involve major structural changes of both the components as revealed by time resolved x-ray diffraction data given in Figure 2b. The peaks appeared at $q = 10.4\ nm^{-1}$ and $q = 11.8\ nm^{-1}$ are, perhaps, related to the crystal structure of $C_1$ and certainly not to that of pure camphor as they disappeared above 130 °C, the temperature at which $C_1$ is seen to be transformed into $C_2$ while, at this composition the solid solution melts around 180 °C.

Peaks centred around $q = 11\ nm^{-1}$ and $q = 12.8\ nm^{-1}$ are observed, that are otherwise very weak for pure camphor and absent for pure $PVF_2$. These peaks probably originated from the solid solution lattice.

Figure 3a illustrates the existence of two incongruently melting polymer-solvent compounds in $PVF_2$-EC binary gel system. From the Tammans plot (plot of gel melting enthalpy as a function of concentration), the stoichiometry of the compounds $C_{1a}$ and $C_{1b}$ can be calculated as $W_{PVF2} = 0.38$. It is to be noted that this concentration does not match with the maximum of the polymer compound melting enthalpies and it is so, perhaps, because of the trapped solvent crystals which are likely to be located in the amorphous domains and are totally absent from the intercalated crystalline domains, hence the occurrence of a solid phase ($S_{sol}$). Below the solvent crystallization temperature, two solid phases therefore occur: a polymer-rich solid phase $S_a$, and a solvent-rich solid phase $S_{sol}$.

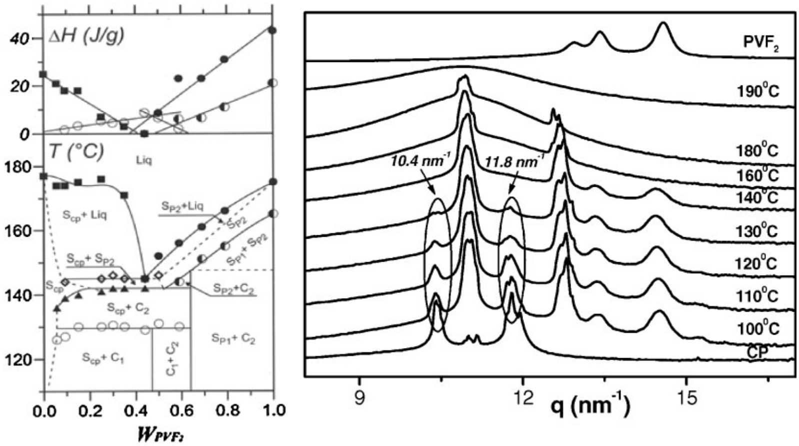

(a) (b)

***Figure 2.***
(a) Phase diagram of $PVF_2$-CP system along with the enthalpy vs composition plot (b) Time resolved WAXD pattern of $PVF_2$-CP gel of composition ($W_{PVF2} = 0.20$).

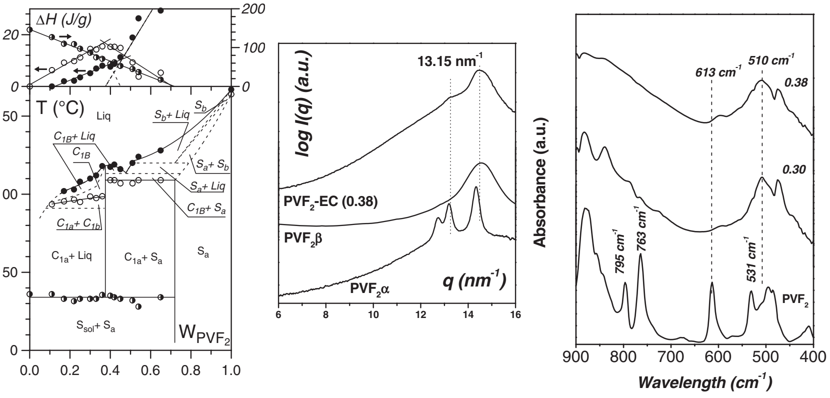

(a) (b) (c)

**Figure 3.**
(a) Phase diagram of $PVF_2$-EC system along with the enthalpy vs composition plot (b) Time resolved WAXD pattern of $PVF_2$-EC gel (c) solvent subtracted FTIR spectra $PVF_2$-EC gel of indicated composition along with that of melt cooled pure $PVF_2$.

In Figure 3b, the WAXD pattern of $PVF_2$-EC gel ($W_{PVF2} = 0.38$) is presented. The reflection maxima appeared at $q = 13.15\ nm^{-1}$ is related to the crystal arrangement of the $PVF_2$-ethylene carbonate molecular compounds. The solvent subtracted FTIR spectra of the same sample along with that of melt cooled $PVF_2$ is presented in Figure 3c and it clearly shows that the $PVF_2$ crystallizes in $\beta$ polymorphic structure while forming the gel.

## Porosity

Figure 4a represents the pore volumes at different pore diameters as found in Mercury Intrusion Porosimetric (MIP) measurement of cyclohexane dried $PVF_2$-DEAZ gel ($W_{PVF2} = 0.10$). The maximum population of mesopores are seen to have pore diameter near to 6 nm but the possibility of pores with diameter lower than 6 nm can not be ruled out. In Figure 4b, the pore size distribution plots

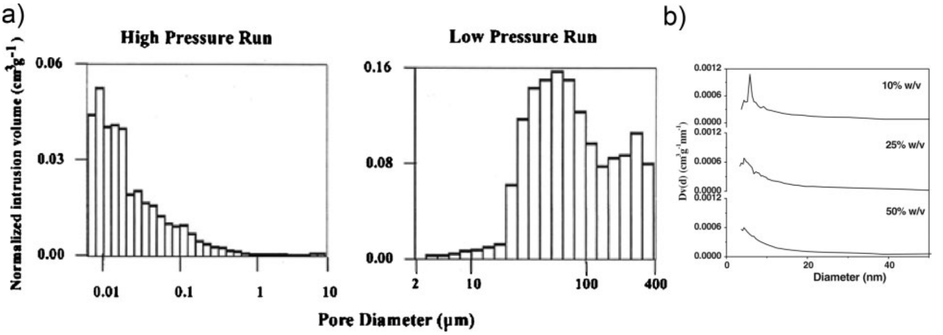

**Figure 4.**
a: MIP pore size distribution of cyclohexane dried $PVF_2$-DEAZ gel ($W_{PVF2} = 0.10$). b: BJH pore size distribution curves of cyclohexane dried $PVF_2$-DEAZ gels at 77 K.

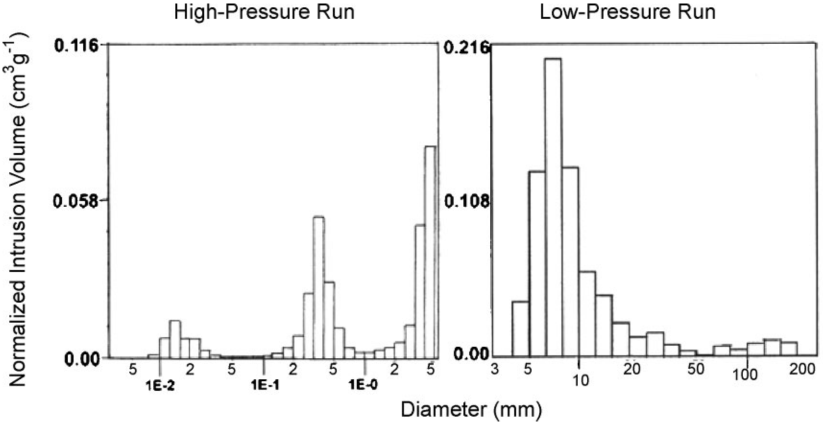

***Figure 5.***
MIP pore size distribution of cyclohexane dried $PVF_2$-CP gel ($W_{PVF2} = 0.40$).

of samples dried from different $PVF_2$-DEAZ gels as obtained in $N_2$ sorption studies are presented. The w/w concentration of the precursor gels are indicated in the figure and it gives only the PSD of mesoporous region.

When $PVF_2$-camphor gel of composition ($W_{PVF2} = 0.40$) for example, is dried with cyclohexane, a sponge like material is obtained and the MIP profile (Figure 5) clearly shows multiporosity thereby reconfirming the feature found in FESEM.

Most surprisingly, we noticed that for a given precursor gel concentration, if camphor is removed by applying vacuum instead of cyclohexane replacement, then the resulting material looses a good amount of surface area (see Table 1). Eventually the decrease in surface is related to some loss of micro and mesoporosity. Figure 6a illustrates the BJH pore size distribution curves for porous $PVF_2$ prepared from the precursor $PVF_2$-CP gel ($W_{PVF2} = 0.10$) by cyclohexane drying (CD) and vacuum drying (VD).

It is apparent from the figure that the distribution function has significantly decreased for VD sample as compared to that of the CD sample and the peak positions also shifted to higher diameter values. This indicates some loss of mesoporosity during removal of solvent (camphor) from the gel by applying vacuum.

Such collapsing of nanostructure is even, more distinct in microporous region as observed in Figure 6b which presents the Horvath-Kawazoe (HK) pore size distributions for the same set of samples. The different peaks may correspond to single double or multiple camphor intercalation. Table 1 summaries the porosity results

***Table 1.***
Pore volume and surface area of cyclohexane dried (CD) and vacuum dried (VD) samples of PVF2-camphor gels.

| Samples | Pore Volume (cm$^3$/g) | | | Surface area (m$^2$/g) | | |
|---|---|---|---|---|---|---|
| | BJH | MIP | | Total | BET | MIP |
| | <6 nm | High pressure | Low pressure | | | |
| P-10 CD | 0.07 | 0.41 | 4.40 | 4.88 | 58.04 | 3.68 |
| P-10 VD | 0.02 | 0.61 | 4.31 | 4.94 | 4.13 | 4.25 |
| P-40 CD | 0.03 | 0.33 | 0.71 | 1.07 | 32.65 | 11.80 |
| P-40 VD | 0.028 | 0.16 | 0.004 | 0.19 | 12.32 | 1.62 |

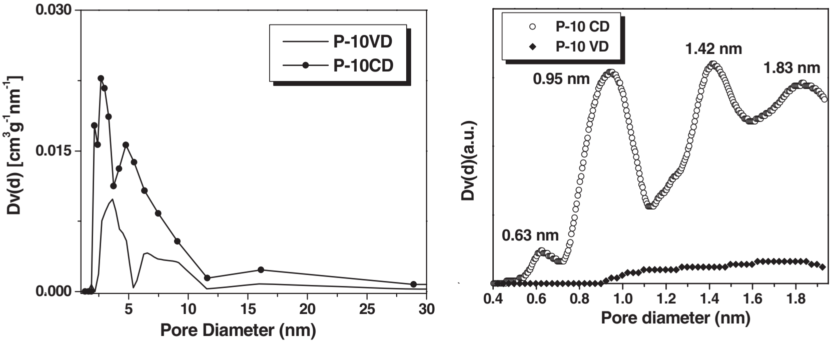

(a) (b)

***Figure 6.***
(a) BJH pore size distribution plots of cyclohexane dried $PVF_2$-CP ($W_{PVF2} = 0.10$) gel (P-10CD) and vacuum dried $PVF_2$-CP ($W_{PVF2} = 0.10$) gel (P-10VD). (b) HK pore size distribution plots for the same set of samples.

for cyclohexane dried and vacuum dried samples prepared from $PVF_2$-CP gels with polymer content $W_{PVF2} = 0.10$ and $W_{PVF2} = 0.40$.

## Conclusion

For poly(vinylidene fluoride)-camphor thermoreversible gel, two incongruently melting polymer-solvent compounds ($C_1$ and $C_2$) are identified with a concurrent formation of a solid solution of $PVF_2$ in camphor as suggested by phase diagram drawn with the aid of Gibbs phase rule. Wide angle X-ray diffraction measurements of the gels show considerable perturbation between the $PVF_2$ and camphor lattices. For $PVF_2$-ethylene carbonate binary system, the existence of polymer solvent compounds $C_{1a}$ and $C_{1b}$ are established by phase diagram and X-ray diffraction studies. WAXD pattern of $PVF_2$-EC gels along with solvent subtracted FTIR spectra confirm the presence of $\beta$ polymorph of $PVF_2$ in gel state. FESEM micrographs of the dried $PVF_2$ gels show foam like porous network with distinct nanofibrils. Porosity results along with scanning electron micrographs conclude successful formation of multiporous materials. Porous $PVF_2$ samples prepared by vacuum drying of $PVF_2$-CP gels show noticeable collapsing of meso and micropores as compared to those prepared with cyclohexane replacement.

*Acknowledgements:* We gratefully acknowledge IFCPAR Grant No. 2808-2 for financial support under excellent category.

[1] A. K. Dikshit, A. K. Nandi, *Macromolecules* **1998**, *31*, 8886.
[2] A. K. Dikshit, A. K. Nandi, *Macromolecules* **2000**, *33*, 2616.
[3] S. Mal, A. K. Nandi, *Macromolecules* **2006**, *39*, 6110.
[4] J. M. Guenet, *Thermoreversible Gelation of Polymers and Biopolymers*, Academic press, London **1992**; J. M. Guenet, *Polymer-solvent Molecular Compounds*, Elsevier, London **2008**.
[5] J. M. Guenet, B. Ray, S. Elhasri, P. Marie, A. Thierry, *NATO Sciences Series 1V: Earth and Environmental Sciences* **2003**, *24*, 191.
[6] S. Malik, D. Roizard, J. M. Guenet, *Macromolecules* **2006**, *39*, 5957.
[7] G. Milano, V. Venditto, G. Guerra, L. Cavallo, P. Ciambelli, D. Sannino, *Chem. Mater.* **2001**, *13*, 1506.
[8] S. A. Davis, S. L. Burkett, N. H. Mendelson, S. Mann, *Nature* **1997**, *385*, 420.
[9] M. Antonietti, B. Berton, C. Göltner, H. Hentze, *Adv. Mater.* **1998**, *10*, 154.
[10] B. T. Holland, L. Abrams, A. Stein, *J. Am. Chem. Soc.* **1999**, *121*, 4308.
[11] D. Zhao, P. Yang, B. F. Chmelka, G. D. Stucky, *Chem. Mater.* **1999**, *11*, 1174.
[12] B. Zhang, S. A. Davis, N. H. Mendelson, S. Mann, *Chem. Commum.* **2000**, 781.
[13] I. Tosheva, V. Valtchev, J. Sterte, *Microporous Mater.* **2000**, *35-36*, 621.

[14] K. H. Rhodes, S. A. Davis, F. Caruso, B. Zhang, S. Mann, *Chem. Mater.* **2000**, *12*, 2832.
[15] L. Huang, Z. Wang, J. Sun, L. Miao, Q. Li, Y. Yan, D. Zhao, *J. Am. Chem. Soc.* **2000**, *122*, 3530.
[16] J. H. Smått, S. Schunk, M. Lindén, *Chem. Mater.* **2003**, *15*, 2354.
[17] A. J. Lovinger, Basset, In *Development in Crystalline Polymers-1*, D. C. Basset, Ed., Elsevier Applied Science, London **1981**, p. 195.
[18] R. E. Newnharn, D. P. Skinner, L. E. Cross, *Mat. Res. Bull.* **1978**, 13. 525.